NUMERICAL APPROXIMATION OF NONLINEAR CHROMATOGRAPHIC MODELS CONSIDERING BI-LANGMUIR ISOTHERM

Ambreen KHAN[a], Sadia PERVEEN[a], Zarmeena SHAHEEN[a], Shamsul QAMAR[b,c]*

[a] Department of Mathematics, AIR University, Islamabad, Pakistan
[b]Department of Mathematics, COMSATS University Islamabad, Pakistan
[c]Max Planck Institute for Dynamics of Complex Technical Systems Magdeburg, Germany

*Corresponding author: sadia.ahsan@mail.au.edu.pk (Sadia Perveen), Tel: +92-51-9261045;

In this research article, two standard models of liquid chromatograaphy, namely the dispersive equilibrium model (DEM) and the kinetic lumped model (KLM) are approximated numerically. We studied the transport of multi components in a single column of chromatography considering non linear adsorption thermodynamics. The models are analyzed for standard Bi-Langmuir and generalized Bi-Langmuir types adsorption equilibrium isotherms using Danckwert (Robin) boundary conditions. Mathematically, the model equations form a non linear system of partial differential equations accounting for the phenomena of advection and diffusion, paired with an algebraic equation or a differential equation for adsorption isotherm. An extended semi-discrete high-resolution finite volume scheme is employed to obtain the approximate solutions of the governing model equations. The method has second to third order accuracy. Several test case studies are conducted to examine the influence of various critical parameters on the process performance. The contemplated case studies incorporate the elution process of liquid chromatography with an increasing number of components. In particular, single component, two component and three component mixtures are considered for the assessment of process performance. The formulated numerical algorithm provide an efficacious mechanism for investigating the retention behavior and the influence of mass transfer kinetics on the shapes of elution profiles.

Key words: *Chromatographic models, Bi-Langumir adsorption isotherm, non equilibrium transport, finite volume method, mass transfer.*

1 Introduction

Chromatography is an efficient and effective technique used in laboratories and industries to separate and analyze many kinds of complex chemical mixtures. This process of separation has been much revolutionized due to the progress in science and technology. Chromatography technique can be effectually employed to target sophisticated segregation tasks for producing high-purity products at the economical production rates. Application areas of chromatography include fine chemical, petrochemical, bio-technical, pharmaceutical, forensic pathology and Nucleic acids research etc. It plays a pivotal part in the realms of forensic testing, finger printing, food and beverage industry, creating vaccinations, DNA testing, insulin purification, plasma fractionation and enzyme purification etc [1–4].

Separation of mixture components through chromatographic methods is based on their selective distribution and various affinities between two non-miscible phases, a flowing liquid known as the mobile phase and a stationary solid phase which is fixed in the column. High performance liquid chromatography (HPLC) apparatus includes a high-pressure pump, a column, an adsorbent (stationary phase), a solvent (mobile phase), a liquid mixture (sample), a computer, a detector, and storage tanks. In this process, the sample of mixture components is fed at the column inlet. The sample components, in contact with the stationary phase, are

transported by the mobile phase throughout the column. They interact distinctly with the stationary phase and thus, migrate through the chromatographic system at different speeds and elute out from the column at different times [3, 4].

A number of dynamical models, taking into consideration diverse levels of complexities, were introduced within literary texts to simulate the over all performance of chromatographic procedures. The frequently considered mass balance chromatographic models are the general rate model (GRM), the non equilibrium kinetic lump model (KLM) and the dispersive equilibrium model (DEM) [1–4]. The physiochemical transport process and the interactions that take place during chromatographic operation are mechanistically represented by a systems of partial differential equations (PDEs). This system is usually paired along some algebraic equations (AEs) or differential equations (DEs) for adsorption isotherm. The linearity and non linearity of these models depend on the adsorption isotherms associated with them. This article deals with the non linear DEM and KLM of chromatography considering Bi-Langmuir sorption isotherms. The analytical solutions of these models are only possible for linear adsorption isotherms which generate decoupled system of equations. As a result, efficient and accurate numerical approximations are needed for predicting dynamical mechanism inside the column [3, 5–7]. Generally, three well known classes of numerical methods have been proposed and applied in the literature for the solution of chromatographic models. The non-oscillatory finite difference (FD) methods like TVB (total variation bounded), TVD (total variation diminishing), ENO (essentially non-oscillatory), and WENO (weighted essentially non-oscillatory), flux limiting finite volume method (FVM) and the discontinuous Galerkin finite element method (DG-FEM) are among the few numerical methods with the ability of resolving discontinuities in the solution profile. [3, 5–12]. The finite volume method (FVM) is an attractive and efficient method that has been widely used to approximate different chromatographic models [5, 6, 13, 14]. The main advantage of the FVM is that the spatial discretization is carried out directly in the physical space. The method is capable to compute weak solutions of the governing equations and narrow peaks of the elution profiles correctly. Moreover, it has the ability to accurately overcome numerical oscillations. The schemes accuracy can be upgraded by introducing high order interpolating polynomials in the solution elements [15–17].

This study extends and generalizes the previous studies of our research group for non-linear DEM and KLM to the case of Bi-Langmuir isotherm [6, 8]. The high resolution finite volume method (HR-FVM) of Koren is extended and utilized for the solutions of governing model equations [17]. The scheme approximates the solution with an accuracy of second to third-order [6, 7]. The spurious oscillations in the solution profiles due to the presence of discontinuities and strong shock waves are resolved numerically by utilizing the flux-limiting functions [6, 17]. A second to third order accurate Runge-Kutta (RK) method is applied to solve the resulting system of ordinary differential equations (ODEs)[18]. Various test problems of single and multi-components elution are examined with a broad range of thermodynamic and kinetic parameters to demonstrate influences of isotherms on the concentration profiles.

The content of this research article are structured in the following manner. In Section 2, the one-dimensional (1D) non linear KLM and DEM are introduced. In Section 3, the proposed HR-FVM is derived for solving KLM. Discussion on the considered numerical case studies to demonstrate the effectiveness of the numerical scheme is presented in Section 4. Conclusion on the basis of result discussion are presented in Section 5.

2 The non linear kinetic lump model (KLM)

In this section, a multi-components nonlinear one dimensional (1D) KLM, is considered to study the effects of band broadening on chromatographic separation process. The KLM is a simple model for the description of mass transfer kinetics inside the chromatographic column. It achieves the mass balances by introducing a kinetic equation that describes the rate of variation of the averaged solute concentration in the stationary phase by assuming a linear driving force. This driving force commenced from the deviation from equilibrium concentration. The model lumps the contributions of external and internal resistances of mass transport into

coefficient of mass transfer. The model assumes that the bed is isothermal and homogeneously packed. It include two fundamental kinetic variables, the coefficient of mass transfer k_{m} and the coefficient of axial dispersion D_z. With these presumptions, the 1D balance equations of mass for the transport of N_c species in the mobile phase can be written as

$$\frac{\partial u_{\mathrm{j}}}{\partial t} + v\frac{\partial u_{\mathrm{j}}}{\partial z} = D_{\mathrm{z,j}}\frac{\partial^2 u_{\mathrm{j}}}{\partial z^2} - \frac{k_{\mathrm{m,j}}(q_{\mathrm{j}}^{*} - q_{\mathrm{j}})}{\epsilon}\,, \quad \text{for} \quad \mathrm{j} = 1, 2, ...N_c\,. \tag{1}$$

Where, N_c denotes the number of species in the sample of mixture, For each component j, $u_{\mathrm{j}}(z,t)$ symbolizes the solute concentration in the mobile phase, the symbol $q_{\mathrm{j}}(z,t)$ denotes the solute concentration in the stationary phase, q_{j}^{*} is the stationary phase concentration in equilibrium, v is the interstitial velocity of mobile phase, $D_{\mathrm{z,j}}$ denotes coefficient of axial dispersion, external porosity of column packing is represented by ϵ, $k_{\mathrm{m,j}}$ is the rate coefficient of mass transfer, while t and z are the time and axial coordinates respectively. The KLM, assumes slow mass transfer kinetics whereas the adsorption desorption kinetics is infinitely fast. Therefore, in addition to the above equation, the associated balance equation for the concentrations of mixture component in the solid particles are also required to complete the model and can be written in the form of kinetic equation as

$$\frac{\partial q_{\mathrm{j}}}{\partial t} = \frac{k_{\mathrm{m,j}}(q_{\mathrm{j}}^{*} - q_{\mathrm{j}})}{1-\epsilon}\,. \tag{2}$$

The equilibrium adsorption isotherm defines an equilibrium relation among the mixture components concentration in the mobile and stationary phases. For modeling and simulation of the chromatographic separation process, it is essential to represent experimentally determined adsorption equilibrium data by suitable mathematical equations. A number of different adsorption isotherm models have been developed in the literature which are classified as linear, Langmuir, BET, and Freundlich isotherms etc [3, 4, 19]. Here, we consider the nonlinear Bi-Langmuir isotherm. This isotherm was derived theoretically by assuming that the surface of adsorbent is covered by two completely independent group of adsorption sites[20–22]. For a mixture of N_c components, the competitive Bi-Langmuir isotherm is expressed as

$$q_{\mathrm{j}}^{*}(u) = \frac{a_{\mathrm{j,I}}u_{\mathrm{j}}}{1+\sum\limits_{\mathrm{k}=1}^{N_c} p_{\mathrm{k}}b_{\mathrm{k,I}}u_{\mathrm{k}}} + \frac{a_{\mathrm{j,II}}u_{\mathrm{j}}}{1+\sum\limits_{\mathrm{k}=1}^{N_c} p_{\mathrm{k}}b_{\mathrm{k,II}}u_{\mathrm{k}}}, \quad \mathrm{k,j} = 1, 2, 3, ...N_c\,, \tag{3}$$

Where j-th component Henry's coefficient is denoted by a_{j}, b_{j} quantizes the extent of non linearity associated with the isotherm, and the symbol p_{j} could have negative or positive signs to indicate the anti-Langmuir behavior and the Langmuir behavior of adsorption isotherm in the components of a mixture. In applications, each mixture component behaves like a Langmuir isotherm if the term p_{j} has a positive sign, other wise it is an anti-Langmuir type. [23, 24]. Moreover, the subscripts I and II refer to the adsorption sites I and II, respectively. The following non dimensional quantities are proposed to facilitate the study:

$$x = \frac{z}{L}, \quad \tau = \frac{vt}{L}, \quad Pe_{\mathrm{z,j}} = \frac{Lv}{D_{\mathrm{z,j}}}, \qquad \kappa_{\mathrm{j}} = \frac{k_{\mathrm{m,j}}L}{v}\,, \tag{4}$$

Here, column length is represented by symbol L, $Pe_{\mathrm{z,j}}$ is the dimensionless Peclet numbers. Substituting the above mentioned dimensionless quantities in the model equations Eqs. (1) and (2), we get

$$\frac{\partial u_{\mathrm{j}}}{\partial \tau} = \frac{1}{Pe_{\mathrm{z,j}}}\frac{\partial^2 u_{\mathrm{j}}}{\partial x^2} - \frac{\partial u_{\mathrm{j}}}{\partial x} - \frac{\kappa_{\mathrm{j}}(q_{\mathrm{j}}^{*} - q_{\mathrm{j}})}{\epsilon}\,, \tag{5}$$

$$\frac{\partial q_{\mathrm{j}}}{\partial \tau} = \frac{\kappa_{\mathrm{j}}(q_{\mathrm{j}}^{*} - q_{\mathrm{j}})}{(1-\epsilon)} \quad 0 \le x \le 1\,. \tag{6}$$

In order to close the model equations Eqs. (5) and (6), appropriate initial conditions (ICs) as well as the boundary conditions (BCs) at the left end and at the right end of the column respectively, must be imposed. We consider an initially equilibrated column i.e

$$u_{\mathrm{j}}(x, \tau = 0) = u_{\mathrm{j}}^{\mathrm{init}}, \quad q_{\mathrm{j}}(x, \tau = 0) = q_{\mathrm{j}}^{*,\mathrm{init}}, \quad \mathrm{j} = 1, 2, 3, ...N_c\,. \tag{7}$$

In this study, we consider rectangular injections and the conventional Danckwerts BCs at the left end of the colum [25]. These BCs are stated as

$$u_j(x=0,\tau) - \frac{1}{Pe_{\mathrm{z,j}}}\frac{\partial u_j(x=0,\tau)}{\partial x} = \begin{cases} u_{\mathrm{j}}^{\mathrm{inj}}\,, & \text{if } 0 \le \tau \le \tau^{\mathrm{inj}}\,, \\ 0\,, & \text{if } \tau > \tau^{\mathrm{inj}}\,, \end{cases} \quad , \quad \mathrm{j} = 1,2,3,.....N_c. \tag{8}$$

These inlet BCs collaborate with Neumann condition at the right end of column

$$\left.\frac{\partial u_{\mathrm{j}}}{\partial x}\right|_{x=1} = 0\,. \tag{9}$$

Where, the j-th component injected concentration is denoted by the symbol $u_{\mathrm{j}}^{\mathrm{inj}}$, the dimensionless time of injection is denoted by τ^{inj}. Moreover, the injection becomes continuous when $\tau^{\mathrm{inj}} \to \infty$ or when the simulation time is less than the injection time τ^{inj}.

2.1 The non linear dispersive equilibrium model (DEM)

The DEM, which is the most simple one among the chromatographic models, assumes that there is permanent equilibrium between the mobile and the stationary phases. Moreover, in DEM, the axial dispersion and all mass transfer resistances because of non equilibrium isotherms are accumulated in an apparent dispersion coefficient. Under these assumptions, D_{z} in Eq. (1) is replaced by a new variable $D^{\mathrm{app,j}} > D_{\mathrm{z}}$. Thus, for instantaneous mass transfer rate i.e $k \to \infty$, Eqs. (1) & (2) can be combined together to obtain the DEM. In dimensionless form,the balance equations of mass, for DEM is

$$\frac{\partial u_{\mathrm{j}}}{\partial \tau} + \mathcal{F}\frac{\partial q_{\mathrm{j}}^*}{\partial \tau} + \frac{\partial u_{\mathrm{j}}}{\partial x} = \frac{1}{Pe_{\mathrm{z,j}}}\frac{\partial^2 u_{\mathrm{j}}}{\partial x^2}\,, \quad \text{for} \quad \mathrm{j} = 1,2,...N_c\,, \tag{10}$$

Where, $\mathcal{F} = \frac{1-\epsilon}{\epsilon}$ symbolizes phase ratio. Eq. (10) assumes the same initial and BCs presented in Eqs. (7), (8) & (9).

3 Numerical method

A number of numerical techniques have been proposed and applied in the literary text for the estimation of the chromatographic models. [3, 6]. In this section, A semi-discrete high resolution flux-limiting finite volume method (HR-FVM) [6, 17] is utilized for the solution the 1D-KLM. The method is easily implementable, compact and simple. It has an accuracy of second to third order in the space variable [8]. The resultant ODEs system is approximated numerically by using a general ODE solver available in the text. The extensive analysis on the accuracy and efficacy of our proposed method has already been done analytically and numerically in the previous articles of our research group [6, 7]. In addition, the method is capable of resolving sharp peaks and discontinuous fronts in the solutions accurately. For the sake of simplicity, we consider a single solute 1D-KLM for the derivation of our proposed numerical method. The method could be easily extended to multi-component combinations in the sample mixture. In the considered single component case, i.e for $u_1 := u$ and $N_c = 1$ Eqs. (5)-(6) becomes:

$$\frac{\partial u}{\partial \tau} = \frac{1}{Pe_z}\frac{\partial^2 u}{\partial x^2} - \frac{\partial u}{\partial x} - \frac{\kappa_{\mathrm{j}}(q^* - q)}{\epsilon}\,, \tag{11}$$

$$\frac{\partial q}{\partial \tau} = \frac{\kappa(q^* - q)}{1-\epsilon}\,. \tag{12}$$

Here, the numerical solution of the PDE in Eq. (11) utilizes the HR-FVM, whereas the ODE given in Eq. (12) is approximated numerically by a standard ODE solver i.e. (ODE23).

Discretization of computational domain: For the implementation of proposed HR-FVM to Eq. (11), the discretization of the computational domain is the initial step. Here, we considered a uniform discretization

of the computational domain $[0,1]$ to avoid intricacy. The mesh intervals width is constant and represented by Δx. Let $\mathcal{N}_x$ be the large integer representing the number of grid point, the coordinate $x_{\mathrm{j}-\frac{1}{2}}$ denotes the mid point for each $\mathrm{j}\,\epsilon\, 1, ..., \mathcal{N}_{x+1}$. The mesh point x_{j} in the interval $\Omega_{\mathrm{j}} \equiv \left[x_{\mathrm{j}-\frac{1}{2}}, x_{\mathrm{j}+\frac{1}{2}}\right]$ are covered by the cell for $1 \leq \mathrm{j} \leq \mathcal{N}_x$.

$$x_{1/2} = 0,\ \ x_{\mathrm{j}+1/2} = \mathrm{j}\Delta x,\ \ x_{\mathcal{N}+1/2} = 1, \tag{13}$$

and

$$x_{\mathrm{j}} = \frac{x_{\mathrm{j}-1/2} + x_{\mathrm{j}+1/2}}{2}, \quad \Delta x_{\mathrm{j}} = x_{\mathrm{j}+1/2} - x_{\mathrm{j}-1/2} = \frac{1}{\mathcal{N}_x + 1}\,. \tag{14}$$

Cell averages: For each cell, the average values of the cell $\nu_{\mathrm{j}}(\tau)$ are defined as

$$\nu_{\mathrm{j}} = \nu_{\mathrm{j}}(\tau) = \frac{1}{\Delta x_j}\int_{\Omega_j} \nu(x,\tau)\, dx\,. \tag{15}$$

Here, $\nu \in \{u, q, q^*\}$. Until now, we have discretized the computational domain and assigned the corresponding initial data set at $\tau = 0$ to each mesh interval.
Integral form of KLM: Assuming that the cell averages ν_{j}^n are provided at the time level τ^n. Then, we can easily find cell averages ν_{j}^{n+1} at the next level of time i.e τ^{n+1}. Integrating Eqs. (11) and (12) over Ω_{j} yields

$$\frac{du_{\mathrm{j}}}{d\tau} = -\frac{u_{\mathrm{j}+\frac{1}{2}} - u_{\mathrm{j}-\frac{1}{2}}}{\Delta x_{\mathrm{j}}} + \frac{1}{Pe_z \Delta x_{\mathrm{j}}}\left[\left(\frac{\partial u}{\partial x}\right)_{\mathrm{j}+\frac{1}{2}} - \left(\frac{\partial u}{\partial x}\right)_{\mathrm{j}-\frac{1}{2}}\right] - \frac{\kappa(q_{\mathrm{j}}^* - q_{\mathrm{j}})}{\epsilon}\,, \tag{16}$$

$$\frac{dq_{\mathrm{j}}}{d\tau} = \frac{\kappa(q_{\mathrm{j}}^* - q_{\mathrm{j}})}{1-\epsilon}\,. \tag{17}$$

The first order derivatives in Eq. (16) can be estimated as

$$\left[\frac{\partial u}{\partial x}\right]_{\mathrm{j}\pm\frac{1}{2}} = \pm\ \left[\frac{u_{\mathrm{j}\pm1} - u_{\mathrm{j}}}{\Delta x_{\mathrm{j}}}\right]. \tag{18}$$

Various numerical schemes can be used to calculate the convective fluxes $u_{\mathrm{j}} \pm \frac{1}{2}$ at the cell interface.
First order numerical method: In this method, the values of concentration are approximated at the cell interfaces in Eq. (16) by utilizing back-ward difference formula. The approximation for concentration can be expressed as

$$u_{\mathrm{j}} = u_{\mathrm{j}+\frac{1}{2}}\,, \qquad u_{\mathrm{j}-1} = u_{\mathrm{j}-\frac{1}{2}}\,. \tag{19}$$

The above mentioned approximations generate a first order accurate method.
The HR-FVM of Koren: Here, the concentration values at the interface of a cell $u_{\mathrm{j}+\frac{1}{2}}$ are approximated by the following flux-limiting formulas [17]:

$$u_{\mathrm{j}+\frac{1}{2}} = u_{\mathrm{j}} + \frac{1}{2}(u_{\mathrm{j}} - u_{\mathrm{j}-1})\zeta\left(\xi_{\mathrm{j}+\frac{1}{2}}\right)\,, \tag{20}$$

where,

$$\xi_{\mathrm{j}+\frac{1}{2}} = \frac{\gamma + u_{\mathrm{j}+1} - u_{\mathrm{j}}}{\gamma + u_{\mathrm{j}} - u_{\mathrm{j}-1}}\,, \tag{21}$$

represent the ratio between successive concentration gradients. Further, to avoid division by zero we consider $\gamma = 10^{-10}$. The limiting function ζ in Eq. (20) can be defined as [17, 26]

$$\zeta\left[\xi_{\mathrm{j}+\frac{1}{2}}\right] = \max\left[0, \min\left[2\xi_{\mathrm{j}+\frac{1}{2}}, \min\left[\frac{1}{3} + \frac{2}{3}\xi_{\mathrm{j}+\frac{1}{2}}, 2\right]\right]\right]\,. \tag{22}$$

Analogously, the concentration $u_{\mathrm{j}-\frac{1}{2}}$ could be computed by changing the index j with the index j $-$ 1.

Other schemes for flux limiting: Different flux limiting methods are accessible from literary material that assume different flux-limiting function [16, 27, 28]. In these schemes, fluxes at the right cell boundary, Ω_j, are expressed as

$$u_{\mathrm{j}+\frac{1}{2}} = u_{\mathrm{j}} + \frac{1}{2}\vartheta\left(\beta_{\mathrm{j}+\frac{1}{2}}\right)\left(u_{\mathrm{j}+1} - u_{\mathrm{j}}\right) . \tag{23}$$

Likewise, we can evaluate the left cell boundary fluxes.Here, $\beta_{j+\frac{1}{2}}$ can be defined as

$$\beta_{j+\frac{1}{2}} = \frac{\gamma + u_{\mathrm{j}} - u_{\mathrm{j}-1}}{\gamma + u_{\mathrm{j}+1} - u_{\mathrm{j}}} . \tag{24}$$

Some well-known flux limiting functions, used in our test problems, are presented in Table 1. The concentration profiles for specific case studies will be analyzed using these flux limiters .

Table 1 – The Flux limiting function used in (23)

Flux-limiter	Formula
MC ([16])	$\vartheta(n) = \max\left(0, \min\left(2n, \frac{1}{2}(1+n), 2\right)\right)$
Superbee ([27])	$\vartheta(n) = \max\left(0, \min(2n, 1), \min(n, 2)\right)$
Minmod ([27])	$\vartheta(n) = \max\left(0, \min(1, n)\right)$
Van Leer ([28])	$\vartheta(n) = \frac{\lvert n\rvert + n}{1+\lvert n\rvert}$

The Stratagem at boundaries of cells: The flux-limiting approximations given by Eqs. (20)-(23) cannot be applied to the boundary element of the cells. Therefore, the first-order backward method is employed to compute cell-interface concentration in the boundary cells. The fluxes at the interfaces of interior cells can be computed by aforementioned second-order accurate HR-FVM.

ODE-solver: A standard ODE solver is utilized for the solution of the ODEs system in Eqs. (16) and (17). Further, the mathematical software "MATLAB" is utilized to program the numerical scheme and the built-in Matlab routine ode23 is utilized to obtain the solution for the resultant ODEs system.

4 Discusion on numerical test problems

Here, the presented HR-FVM is applied to simulate different chromatographic elutions. In the numerical test cases, chromatographic elutions are considered for a) single component 1D DEM and 1D KLM b) two components 1D KLM, and c) three-component 1D LKM, respectively. For the sake of simplicity, the axial dispersion coefficients $D_{\mathrm{z,j}} = D_{\mathrm{z}}$ and the mass transfer coefficients $k_{\mathrm{m,j}} = k_{\mathrm{m}}$, for $j = 1, 2, \cdots, \mathcal{N}_c$, are supposed to be identical in all components. However, for practical applications the current model equations allow different values for these kinetic parameters for each component.

4.1 The single component elution

At the current sub-section, few test cases are discussed for non linear single component elution. We analyze the single component 1D-DEM given by Eq. (10) and 1D-KLM given by Eqs. (11) and (12) for standard Bi-Langmuir non linear isotherm $q^*(u) = \frac{a_{1,\mathrm{I}}u}{1+b_{1,\mathrm{I}}u} + \frac{a_{1,\mathrm{II}}u}{1+b_{1,\mathrm{II}}u}$ with $p_{\mathrm{j}} = 1$ in Eq. (3). Both continuous (Left plots) and pulse (right plots) injections are taken into account. The Dankwerts BCs given in Eqs. (8) & (9) are employed. Table 2 reflect the standard parameters utilized in this case study.

Effects of injected concentration: Figures 1 displays the effects of finite-width injected concentrations. Here, four distinct injected volumes, such as $u^{\mathrm{inj}} = 1\,g/l$, $u^{\mathrm{inj}} = 4\,g/l$, $u^{\mathrm{inj}} = 7\,g/l$ and $u^{\mathrm{inj}} = 10\,g/l$ are

Table 2 – Standard parameters utilized in single-component elution.

Parameters	L [cm]	ϵ [-]	v [cm/min]	D_z [cm^2/min]	t_{inj} [min]	$t_{\max}$ [min]	u^{init} [g/l]	u^{inj} [g/l]	$a_{1,\text{I}}$ [-]	$a_{1,\text{II}}$ [-]	$b_{1,\text{I}}$ [-]	$b_{1,\text{II}}$ [-]
values	1	0.4	0.1	0.0001	2	60	0	10	0.5	1.0	0.05	0.1

taken into consideration in an initially empty column i.e $u^{\text{init}} = 0\,g/l$. The sample pulse is infused into the column for $t^{\text{inj}} = 12\,min$. The plots reveals that the peak heights start improving by increasing the volume of feeded concentration. It depicted the well known fact that the band width is proportional to the volume of injected sample. The concentration profiles for DEM have sharp and narrow peaks representing equilibrium, where as the profiles have broader fronts for the KLM for the considered small value of dimension less rate coefficient of mass $k = 1\,min^{-1}$. It could be observed from these plots that the column with-holding time is decreased with the rising value of injected concentration. The self sharpening effects of adsorption fronts becomes discernible for both models.

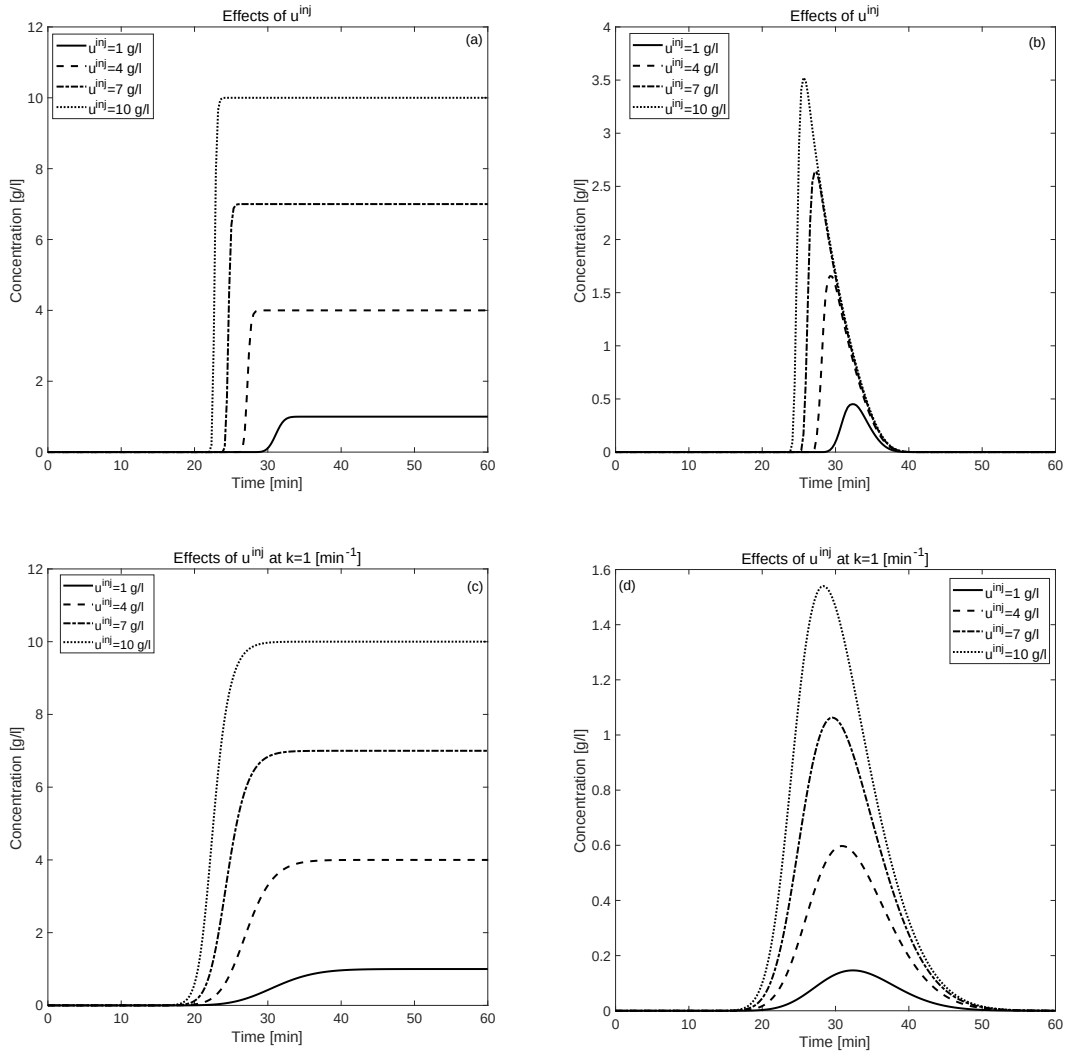

Figure 1 – Effects of injected concentration u^{inj} for nonlinear single-component elution: (a,b) for DEM (c,d) for KLM with Danckwert BCs.

Effects of velocity: Figure 2 compares the concentration profiles for DEM (plot (a) & (b)) and KLM (plot (c) & (d)) to study the impact of flow-rate on retention time. Again the profiles are plotted for both continuous and pulse injections. Four different flow rates $v = 0.1\,cm/min$, $v = 0.15\,cm/min$, $v = 0.2\,cm/min$, and $v = 0.25\,cm/min$ are considered for the same value of $t^{\text{inj}} = 2\,min$. Notably, the peak height with KLM is smaller than the DEM, becasue of delay in adsorption process incorporated in the model. It has also been observed that the column with holding time significantly reduces with the increase in the interstitial velocity. Moreover, the profiles become sharp with the dominant effects of considered adsorption for higher value of velocity and vice versa.

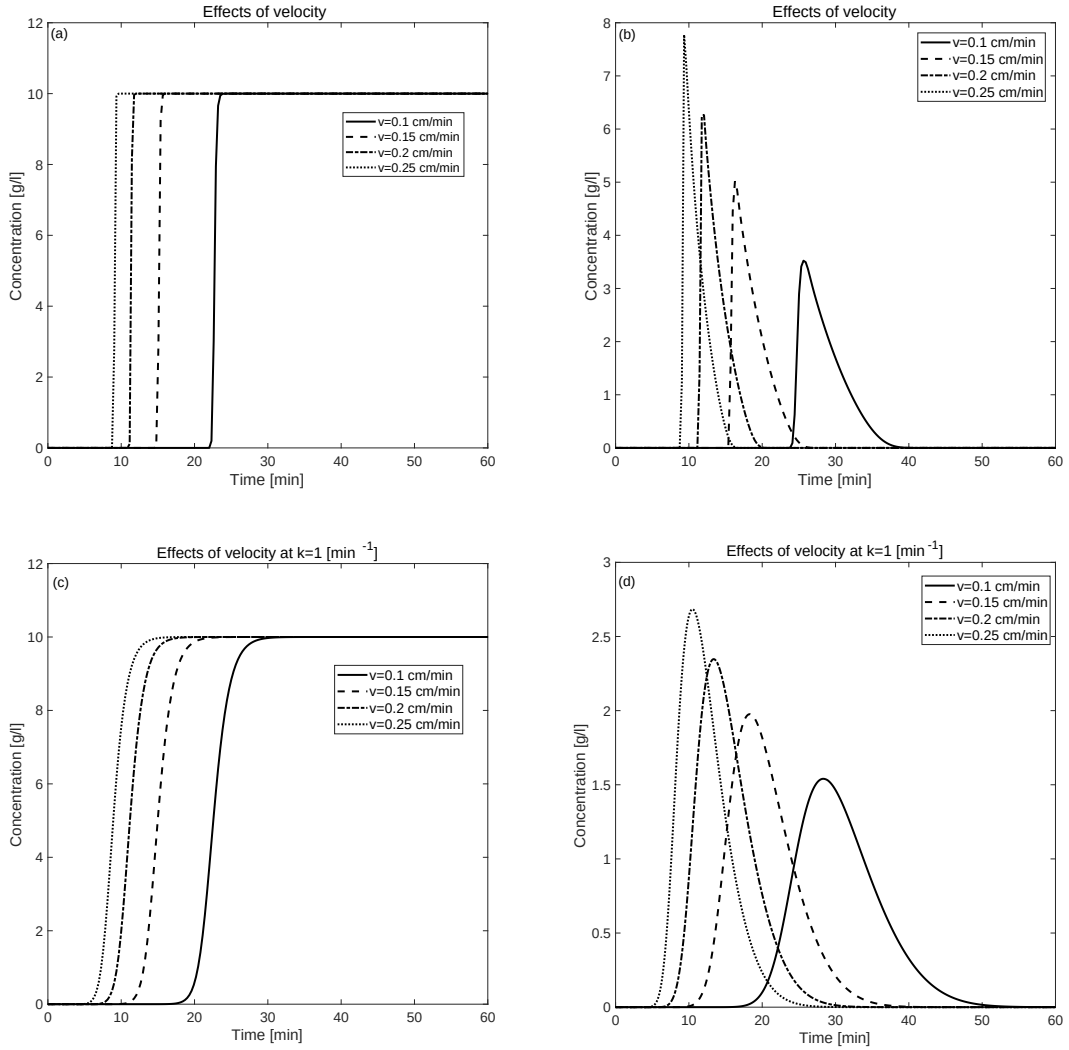

Figure 2 – Effects of varying velocity for nonlinear single component elution: (a,b) for EDM (c,d) for LKM with Danckwert BCs.

Effects of mass transfer coefficient: Figure 3 exhibits the influence of mass transfer coefficient k on 1D-KLM. The characteristic effects of nonlinear isotherm (Bi-Langmuir) are clearly evident from this figure. The profile is diffusive and broad for small value of $k = 1\,min^{-1}$ and produces sharp corner for larger value of $k = 100\,min^{-1}$. For $k = 100\,min^{-1}$ the solution of KLM reduces to that of DEM as depicted in figure 4. On the other hand, for small value of $k\,min^{-1}$, the solution of KLM largely differs from the condition of equilibrium and hence, from the solution of DEM.

Relative error for KLM: Here, the single component KLM (c.f. Eq. (1) & (2)) together with the Bi-Langmuir non linear isotherm $q^*(u) = \frac{a_{1,\mathrm{I}}u}{1+b_{1,\mathrm{I}}u} + \frac{a_{1,\mathrm{II}}u}{1+b_{1,\mathrm{II}}u}$ with $p_j = 1$ in Eq. (3) is considered to compute relative errors. The standard parameters used in this problem are displayed in Table 2. However, the experimental order of convergence and the accuracy of the method has already been computed in the previous articles by our research group [7, 8]. In the absence of analytical solution for the considered non linear PDEs, the solution of the flux-limiting Koren method at 3000 grid points is taken as the reference solution. The numerical solutions for 100 computational grid points at the column outlet are compared with the reference solution for $k = 1\,min^{-1}$ & $k = 100\,min^{-1}$ as shown in Figure 4.

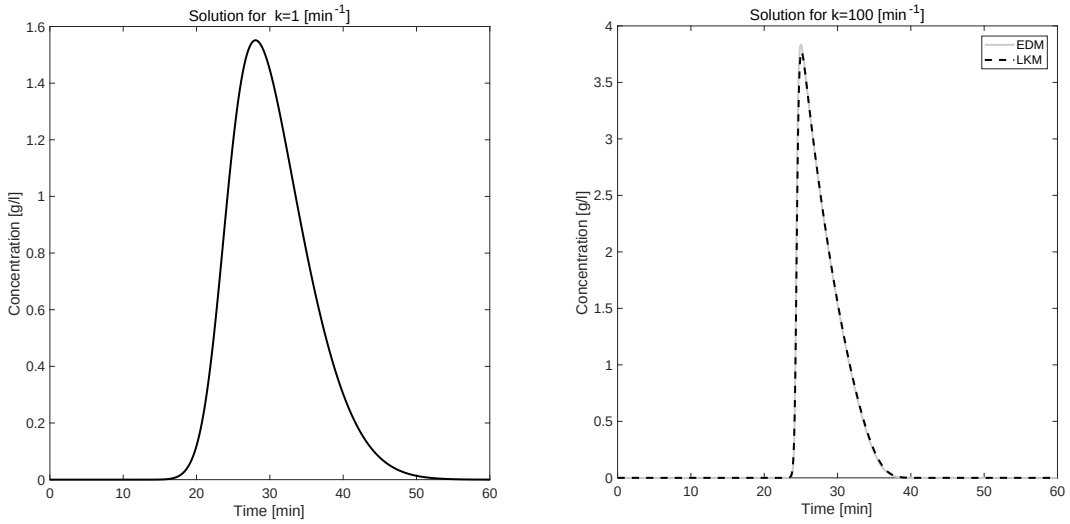

Figure 3 – Effect of mass transfer coefficient $k\,[min^{-1}]$ on nonlinear single component elution.

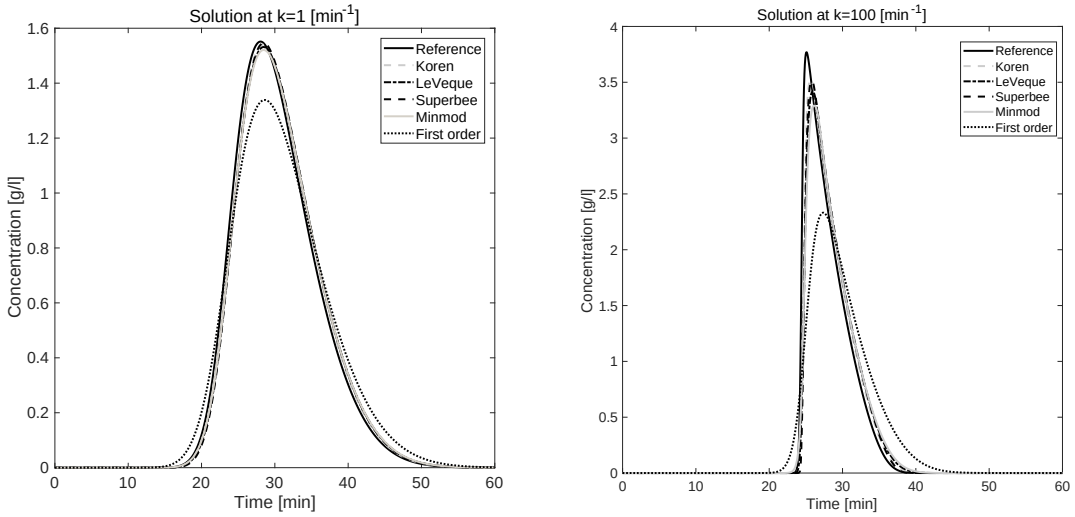

Figure 4 – Comparison of scheme for non-linear single component elution.

The relative error in time at the outlet of column ($x = 1$) can be calculated using the formula

$$\text{Relative error} = \frac{\sum_{n=1}^{N_T} |U_R^n - U_N^n|}{\sum_{n=1}^{N_T} |U_R^n|}, \tag{25}$$

Here, $U_R^n := U_R^n(x = 1, \tau)$ represents the reference solution at time τ^n and $U_N^n(x = 1, \tau)$ is the corresponding numerical solution. N_T denotes the total number of time steps and $\Delta\tau$ denotes the size of time step. Table 3 exhibits the relative error and experimental order of convergence (EOC) calculated by using Koren method for various grid points by assuming D_z as a variable . The results in table 3 depicts that the suggested flux limiting Koren scheme is second order acurate. The relative-errors and CPU run-times of different numerical schemes is computed in table 4, for two distinct values of $k = 1\,min^{-1}$ and $k = 100\,min^{-1}$ at 100 grid point. Notably, the Koren method generates smaller error in comparison to the other schemes in terms of precision and efficacy. The solutions are smooth and have diffusive profile for $k = 1\,min^{-1}$. Thus, all the considered flux-limiting methods produces equivalent errors. Further, the first order method produced a diffusive profile, while the predicted concentration profiles of other schemes are in good agreement.

Table 3 – Relative-error and EOC of the Koren scheme for single component elution.

Grid points	$D_z = 0.001$		$D_z = 0.0001$		$D_z = 0.00001$	
	Relative-error	EOC	Relative-error	EOC	Relative-error	EOC
100	0.0437		0.0493		0.0507	
200	0.0226	0.9513	0.0237	1.0567	0.0240	1.0790
400	0.0111	1.0258	0.0112	1.0814	0.0110	1.1255
800	0.0048	1.2095	0.0050	1.1635	0.0046	1.2578
1600	0.0016	1.5850	0.0017	1.5564	0.0015	1.6167
3200	1.1337×10^{-4}	3.8190	1.2427×10^{-4}	4.0875	1.0373×10^{-4}	3.9069

Table 4 – Relative-errors and CPU run times for single component elution considering Bi-Langumir isotherm at 100 grid points.

flux Limiters	Relative-error		CPU(s)
	$k = 1\,min^{-1}$	$k = 100\,min^{-1}$	
Superbee	0.0732	0.1805	11
Koren	0.0493	0.1296	10
van Leer	0.0705	0.1808	10
MC	0.0711	0.1833	10
Minmod	0.0686	0.1955	9
First order	0.1458	0.4526	6

4.2 The Two component elution

In this subsection, we have extended our analysis for the two component non linear elution. In these case studies, the numerical results are generated by solving two component non-equilibrium 1D-KLM with the HR-FVS of Koren [6, 17]. Once again the analysis is done by using the Danckwert BCs for infinite and finite feed volumes.

Case I [Generalized Bi-Langmuir isotherm]: In this specific study, 1D-KLM given in Eq. (1) & (2) along with generalized Bi-Langmuir isotherms with $p_1 = -1$ & $p_2 = 1$ in Eq. (3) are used to simulate the propagation of a mixture carrying two components through a chromatographic column [23, 24]. All the standard parameters needed in the simulation are listed in Table 5.

Table 5 – Case I:[Generalized bi-Langmuir isotherm (Parameters of nonlinear two-component LKM].

Parameters	L [cm]	ϵ [-]	v [cm/min]	D_z [cm^2/min]	$a_{1,\mathrm{I}}$ [-]	$a_{1,\mathrm{II}}$ [-]	$a_{2,\mathrm{I}}$ [-]	$a_{2,\mathrm{II}}$ [-]	$b_{1,\mathrm{I}}$ [-]	$b_{1,\mathrm{II}}$ [-]	$b_{2,\mathrm{I}}$ [-]	$b_{2,\mathrm{II}}$ [-]
values	1	0.4	0.1	0.000001	0.5	0.75	0.25	2.0	0.05	0.015	0.0001	0.1

The column is set at a constant initial state in accordance with a certain initial composition. A specific feed composition is continuously injected in the column at time $\tau = 0$ for producing an inlet state. For small axial dispersion coefficient, this set-up coincides to a specific Riemann-problem.

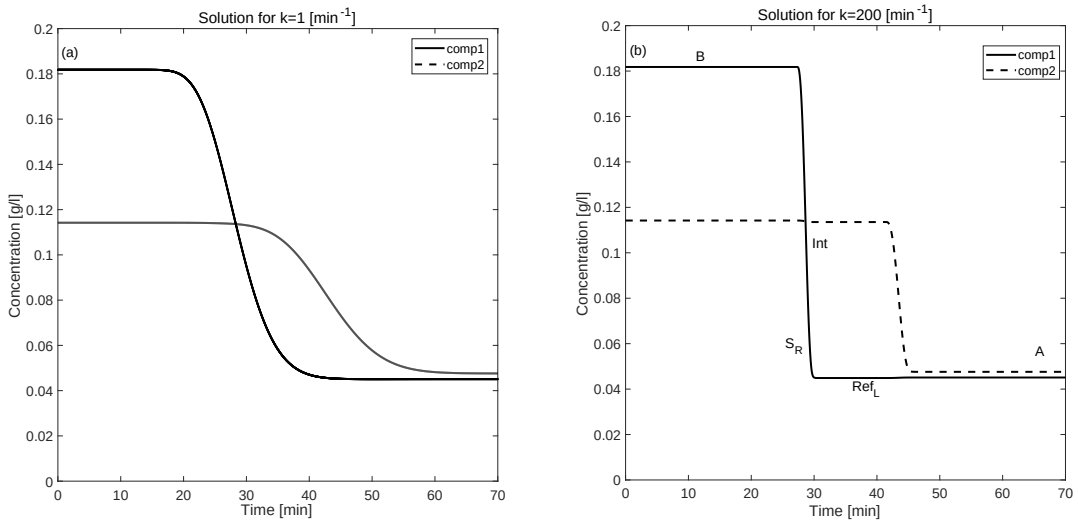

Figure 5 – Plots of Case I (Riemann Problem) at the column outlet

.

In non linear chromatographic theory, solutions of Riemann-problem are classified into three different elution fronts. These elution fronts are characterized as a semi-shock wave, a shock wave (discontinuous) and simple rarefaction wave (continuous). Shock is defined as a mathematical discontinuity in the equilibrium theory of non linear chromatography. Shock waves arise when upstream state of composition fronts propagate faster than the downstream state. As a consequence of this compression, shock waves has sharp front and the components concentration improves across the shock. Contrary to the shock waves, rarefaction waves are the waves of expansion through which concentration decreases. They typically occur when the mobile phase eluted a strongly retained component, as the composition fronts travel along the column.
The numerical solutions comprises of three constant states, for instance the inlet state $\mathcal{A}$ is defined on the left, the initial state $\mathcal{B}$ is defined on the right, parted by two waves of transition which might be either the shock waves or the simple waves and the intermediate state (*Int*) is at the intercept of the characteristics of different index arising from states $(\mathcal{A})$ and $(\mathcal{B})$ respectively. In addition, we used the following abbreviations in the plot: $\mathcal{S}_{\mathcal{R}}$:= shock wave on the right, and $Ref_{\mathcal{L}}$:= rarefaction wave on the left.
Result for the simulation of Case I: The following set of parameter values is used to perform the considered simulation by our suggested numerical method. The inlet concentrations for the component I is taken as $u_1^{\mathrm{inj}} = 0.0451\, g/l$ and for the component II is $u_2^{\mathrm{inj}} = 0.0476\, g/l$. The initial concentrations for component I is taken as $u_1^{\mathrm{init}} = 0.1818\, g/l$ and for the component II is $u_2^{\mathrm{init}} = 0.1142\, g/l$. The injection time for the problem is $t^{\mathrm{inj}} = 2.0\ min$ and the total time of simulation is $t^{\max} = 80\, min$. The numerical predictions in time for two different values of k at the column out let i.e. $x = 1$ are displayed in Figure 5. The plots in Figure 5 leads to the classical solution. The solution has two constant states namely the initial state $(\mathcal{B})$ on

right and the inlet state $(\mathcal{A})$ on left respectively, a shock wave on the right $\mathcal{S}_{\mathcal{R}}$, an intermediate state (Int) in the center, and a rarefaction wave on the right $Ref_{\mathcal{L}}$. It was observed that for the considered smaller value of $k = 1\,min^{-1}$ the solution fronts are more diffusive in comparison of the solution front for the large value of $k = 200\,min^{-1}$. Moreover, when $D_z \to 0$ the solutions fronts would become more steep and sharper.

Case II [Standard Bi-Langmuir isotherm]: In this test case, 1D-KLM given in Eqs. (1) and (2) is applied to the two component chromatographic model i.e $N_c = 2$. The standard non linear Bi-langumir isotherm with $p_1 = p_2 = 1$ in Eqs. (3) is taken into consideration for specific injected volumes. The optimal parameters needed for the solution of the problem are $L = 1\,cm$, $v = 0.1\,cm/min$, $\epsilon = 0.4$, $a_{1,\mathrm{I}} = 0.5$, $a_{1,\mathrm{II}} = 0.75$, $a_{2,\mathrm{I}} = 0.25$, $a_{2,\mathrm{II}} = 2.0$, $b_{1,\mathrm{I}} = 0.05$, $b_{1,\mathrm{II}} = 0.015$, $b_{2,\mathrm{I}} = 0.0001$, $b_{2,\mathrm{II}} = 0.1$, $t^{\max} = 80$ min and $D_{\mathrm{z,i}} = 0.0001\,cm^2/min$. A rectangular pulse of the liquid mixture containing the two components $u_{\mathrm{i}}^{\mathrm{inj}} = 1\,g/l$ is infused in the flowing stream of solvent for $t^{\mathrm{inj}} = 12\,min$. The Dankwerts BCs given by Eqs. (8) & (9) for $N_c = 2$ are utilized to generate the numerical result. In Figures 6, numerical predictions for two distinct values of rate coefficient of mass transfer k are shown. It is depicted from the Figure 6 that the concentration profiles become broaden along with elongated tails for $k = 1\,min^{-1}$. Whereas, for $k = 100\,min^{-1}$ the concentration profiles of both components show improvement in separation and have narrow rectangular shapes. Moreover, for $k = 100\,min^{-1}$, the results of KLM are exactly equivalent to those obtained for DEM.

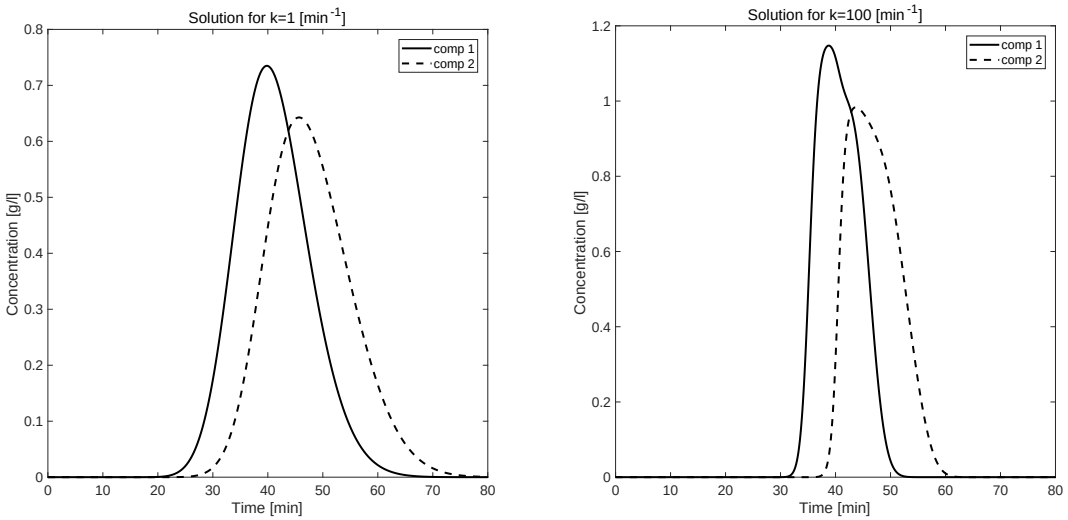

Figure 6 – Two component non-linear elution profile at the column outlet

.

The effects of non equimolar injection are demonstrated in Figure 7. Three different injection volumes such as (a). $u_1^{\mathrm{inj}} = 6\ g/l$ & $u_2^{\mathrm{inj}} = 3\ g/l$, (b). $u_1^{\mathrm{inj}} = 4\ g/l$ & $u_2^{\mathrm{inj}} = 2\ g/l$, (c). $u_1^{\mathrm{inj}} = 1\ g/l$ & $u_2^{\mathrm{inj}} = 0.5\ g/l$, respectively are investigated. Once again the numerical results are generated for two different values of the rate coefficient of mass k. The elution profiles are diffusive for $k = 1\,[min^{-1}]$, the diffusion process dominates the convection process and due to the considered small value of mass transfer coefficient the equilibrium is not achieved. Whereas for $k = 1000\,[min^{-1}]$, the profiles are sharp and peaked, the results depict equilibrium in the phase system. Moreover, for $k = 1000\,min^{-1}$, it can be observed that, an increase in the volume of injected feed produces an overshoot in the concentration profiles. Moreover, the prominent impact of self-sharpening fronts of adsorption can be observed.

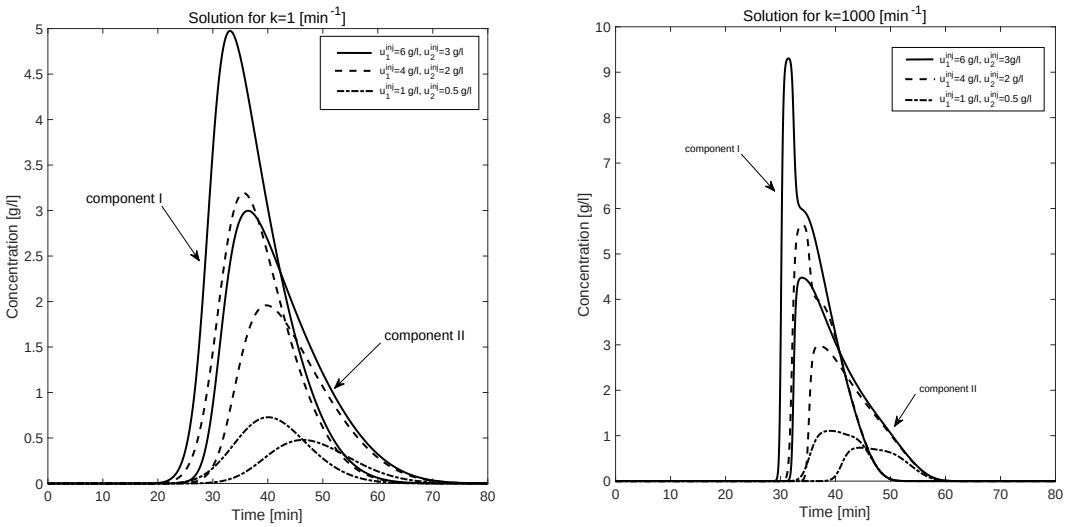

Figure 7 – Effects of non-equimolar injection on two component non linear elution profiles for $k = 1\,[min^{-1}]$ and $k = 1000\,[min^{-1}]$.

.

4.3 The three component elution

Figure 8 presents the elution profiles for a three component segregation process. The parameters for the solution of this case study are $L = 1\,cm$, $\epsilon = 0.4$, $v = 0.1\,cm/min$, $a_{1,\mathrm{I}} = 1.0$, $a_{1,\mathrm{II}} = 0.75$, $a_{2,\mathrm{I}} = 0.5$, $a_{2,\mathrm{II}} = 2.0$, $a_{3,\mathrm{I}} = 0.25$, $a_{3,\mathrm{II}} = 3.5$, $b_{1,\mathrm{I}} = 0.05$, $b_{1,\mathrm{II}} = 0.015$, $b_{2,\mathrm{I}} = 0.0001$, $b_{2,\mathrm{II}} = 0.1$, $b_{3,\mathrm{I}} = 0.02$, $b_{3,\mathrm{II}} = 1.0$, $t^{\max} = 100$ min and $D_z = 0.0001\,cm^2/min$. Numerical simulation are computed for standard Bi-Langmuir isotherm given in Eq. (3), for j $= 1, 2, 3$. The inlet concentration of height $u_{\mathrm{j}}^{\mathrm{inj}} = 1\,g/l$ for j $= 1, 2, 3$ is infused into column with initial concentration $u_{\mathrm{j}}^{\mathrm{init}} = 0\,g/l$ for $t^{\mathrm{inj}} = 2\,min$. The numerical results generated for two distinct values of rate coefficient k of the mass transfer are displayed in 8. The numerical predictions depicts asymmetrical, sharp fronts which is a typical behavior of Bi-Langmuir adsorption isotherm. further, components with greater value of equilibrium constant of adsorption elute later from the column and the components having smaller values of equilibrium constant of adsorption elute early. The generated elution profiles are dispersed and tailed for $k = 1\,min^{-1}$. Moreover, a better separation is accomplished as a result of the establishment of equilibrium for sufficiently large value of k (i.e for $k = 100\,min^{-1}$).

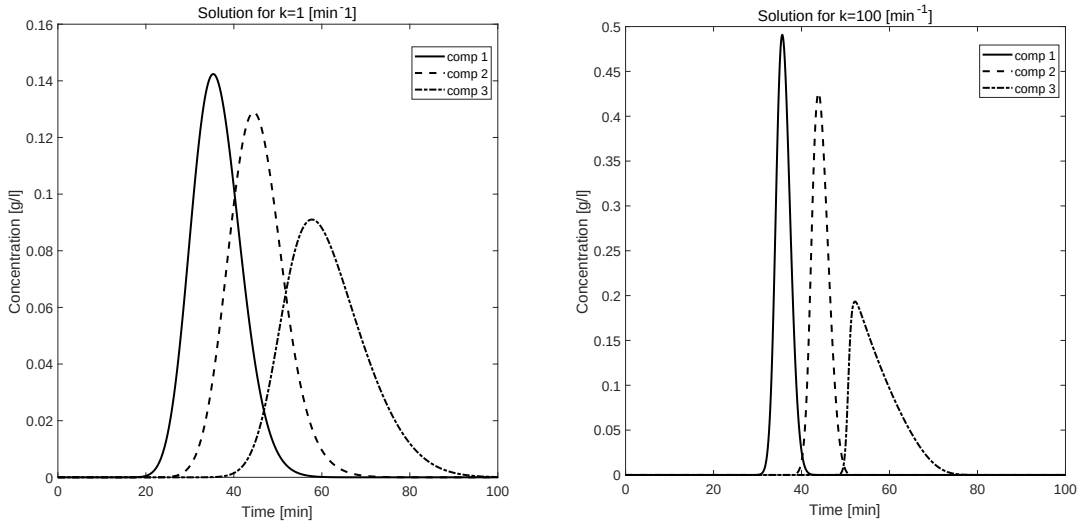

Figure 8 – Three component non linear elution profiles

.

5 Conclusion

In this article, two dynamic models known as dispersive equilibrium and the kinetic lump models of liquid chromatography are simulated numerically. The considered chromatographic models were examined for the Bi-Langmuir adsorption isotherm by using Danckwert boundary conditions. The resulting systems consists of advection-diffusion partial differential equations paired with an algebraic or the differential equation. A high resolution flux-limiting finite volume method was extended for the numerical solutions of the considered models. Numerous case studies of increasing difficulty, includes (a) single component, (b) two component, and (c) three component elution were considered to scrutinize the models. The effects of various kinetic parameter, in particular the rate coefficient of mass transfer and the effects of injected feed volumes, were studied on the performance of process. Further, the concentration profiles were investigated over nonlinear chromatographic conditions for a broad variety of flux limiting functions. The presented finite volume gives second order accuracy. The scheme avoids over predictions and numerical oscillations in the solutions. The performance of the scheme in terms of stability, accuracy and computational time was validated against other flux limiting finite volume schemes. The suggested scheme was found more suitable on the basis of simulation results. Although this article deals with 1D dispersive equilibrium and the kinetic lump models under isothermal conditions, the analysis can be expanded to the models with enhanced resistance of mass transfer and reaction operating under non-isothermal conditions. Moreover, the analysis could also be extended to 2D models in various situations. Such simulations are advantageous for better understanding of underlying transport mechanisms, up-grading physiochemical parameters and optimizing the experimental conditions.

Nomenclature

$a_{i,\mathrm{I}}$	-Adsorption constant of component i for site I , $[-]$	$\mathcal{F}$	-Phase ratio, $[-]$
$a_{i,\mathrm{II}}$	-Adsorption constant of component i for site II, $[-]$	k_{m}	-Mass transfer coefficient, $[min^{-1}]$
$b_{i,\mathrm{I}}$	-Bi-Langmuir isotherm coefficient of component i for site I , $[-]$	z	-Axail coordinate, $[-]$
$b_{\mathrm{i,II}}$	-Bi-Langmuir isotherm coefficient of component i for site II , $[-]$	t	-Time coordinate, $[min]$
$u_{\mathrm{j}}^{\mathrm{init}}$	-Initial concentrations, $[g/l]$	v	-Intersticial phase velocity, $[cm/min]$
$u_{\mathrm{j}}^{\mathrm{inj}}$	-Inlet concentration, $[g/l]$	t^{inj}	-Time of injection, $[-]$
$D_{\mathrm{z,j}}$	-Axial Dispersion coefficient, $[cm^2/min]$	t^{max}	-Total simulation time, $[min]$
ϵ	-External porosity, $[-]$	L	-Column length, $[cm]$

References

[1] Guiochon, G., Preparative liquid chromatography, *J. Chromatogr. A* ., *965* (2002), pp. 129-161.

[2] Guiochon, G., Lin, B., *Modeling for preparative chromatography*, Academic Press., Amsterdam, 2003.

[3] Guiochon, G., Felinger, A., Shirazi, D. G., Katti, A.M., *Fundamentals of preparative and nonlinear chromatography*, 2nd ed., ELsevier Academic press, New York, 2006.

[4] Ruthven, D.M., *Principles of Adsorption and Adsorption Processes*, John Wiley and Sons, Wiley-Interscience, New York, 1984.

[5] Lieres, E.V., Andersson, J., A Fast and accurate solver for the general rate model of column liquid chromatography, *J. Comput. & Chem. Eng*., *34*, (2010), 8, pp. 1180-1191.

[6] Javeed, S., Qamar, S., Seidel-Morgenstern, A., Warnecke, G., Efficient and accurate numerical simulation of nonlinear chromatographic processes, *J. Comput. Chem. Eng*., *35*, (2011), 11, pp. 2294-2305.

[7] Qamar, S., Perveen, S., Seidel-Morgenstern, A., Numerical approximation of nonlinear and non-equilibrium two-dimensional model of chromatography, *J. Comput. Chem. Eng*., *94*, (2016), pp. 411-427.

[8] Javeed, S., Qamar, S., Seidel-Morgenstern, A., Warnecke, G., A discontinuous Galerkin method to solve chromatographic models, *J. Chromatogr. A*., *1218*, (2011), 40, pp. 7137-7146.

[9] Püttmann, A., Nicolai, M., Behr, M., von Lieres, E., Stabilized space-time finite elements for high-definition simulation of packed bed chromatography, *Finite Elem. Anal. Des*., *86*, (2014), pp. 1-11.

[10] Püttmann, A., Schnittert, S., Leweke, S., von Lieres, E., Utilizing algorithmic differentiation to efficiently compute chromatograms and parameter sensitivities, *Chem. Eng. Sci*., *139*, (2016), pp. 152-162.

[11] Qamar, S., Sattar, F.A., Abbasi, J.N., Seidel-Morgenstern, A., Numerical simulation of nonlinear chromatography with core-shell particles applying the general rate model, *Chem. Eng. Sci*., *147*, (2016), pp. 54-64.

[12] Rouchon, P., Schonauer, M., Valentin, P., Guiochon, G., Numerical Simulation of Band Propagation in Nonlinear Chromatography, *Sep. Sci. Technol*., *22*, (1987), 8-10, pp. 1793-1833.

[13] Cruz, P., Santos, J.C., Magalhães F.D., Mendes, A., Simulation of separation processes using finite volume method, *J. Comput. & Chem. Eng*., *30*, (2005), 1, pp. 83-98.

[14] Webley, P.A., He, J., Fast solution-adaptive finite volume method for PSA/VSA cycle simulation; 1 single step simulation, *J. Comput. & Chem. Eng*., *23*, (2000), 11-12,pp. 1701-1712.

[15] LeVeque, R.J., *Numerical methods for conservation laws*, Birkhaüser Verlag, Bassel, Germany, 1992.

[16] Leer, B.V., Towards ultimate conservative finite difference scheme.IV. A new approach to numerical convection. scheme, *J. Comput. Phys*., *23*, (1997), 3, pp. 276-299.

[17] Koren, B., A robust upwind discretization method for advection, diffusion and source terms, Notes on Numerical Fluid Mechanics, chapter 5, in: *Numerical Methods for Advection-Diffusion Problems*, C.B. Vreugdenhil, B. Koren, Vieweg Verlag, Braunschweig, *45*, 1993, pp. 117-138

[18] S. Gottlie., C.-W. Shu., Total Variation Diminishing Runge-Kutta Schemes, *Mathematics of Computation*., *67*, (1998), 221, pp. 73-85.

[19] Dondi, Francesco., Guiochon, G., *Theoretical Advancement in Chromatography and Related Separation Techniques*, Springer Science+Business Media Dordrecht., Ferrara, Italy, 1992.

[20] Ortner, F., Jermann, S., Joss, L., Mazzotti, M., Equilibrium Theory Analysis of a Binary Chromatographic System Subject to a Mixed Generalized Bi-Langmuir Isotherm., *Ind. Eng. Chem. Res*., *54*, (2015), 45, pp. 11420–11437.

[21] Gritti, F., Guiochon, G., Analytical Solution of the Ideal Model of Chromatography for a Bi-Langmuir Adsorption Isotherm., *Anal. Chem*., *85*, (2013), 81, pp. 8552-8558.

[22] Demin. A. A., Melenevsky.T.A., Bi-Langmuir Isotherms' Applicability for Description of Interaction of Ion-Exchange Sorbents with Protein Mixtures., *J. Chromatogr. Sci.*., *44*, (2006),pp. 181-186.

[23] Mazzotti, M., Local equilibrium theory for the binary chromatography of species subject to a generalized langmuir isotherm *Ind. Eng. Chem. Res*., *45*, (2006), 15, pp. 5332-5350.

[24] Mazzotti, M., Nonclassical composition fronts in nonlinear chromatography: Delta-shock. *Ind. Eng. Chem. Res*., *48*, (2009),16, pp. 7733-7752.

[25] Danckwerts, P.V., Continuous flow system Distribution of residence times, *J. Chem. Eng. Sci*., *2*, (1953), 1, pp. 1-13.

[26] Sweby, P.K., High resolution schemes using flux limiters for hyperbolic conservation laws, *SIAM J. Numer. Anal.*, *21*, (1984), 5, pp. 995-1011.

[27] Roe, P.L., Characteristic-based schemes for the Euler equations, *Annual Review of Fluid Mechanics*., *18*, (1986), pp. 337-365.

[28] Leer, B.V., Towards ultimate conservative finite difference scheme.2. Monotonicity and conservation combined in a second-order scheme, *J. Comput. Phys*., *14*, (1974), 4, pp. 361-370.

[29] Kondrat, S., Zimmermam, O., Wiechert, W., von-Lieres, E., Discrete-continuous reaction-diffusion model with mobile point-like sources and sinks, *Eur. Phys. J. E*., *39*, (2016), 1, pp. 11.

[30] Leweke, S., von-Lieres, E., Fast arbitrary order moments and arbitrary precision solution of the general rate model of column liquid chromatography with linear isotherm, *Comput & Chem. Eng*., *84*, (2015), pp. 350-362.

[31] Ghosh, P., Vahedipour, K., Leuthold, M., von-Lieres, E., Model-based analysis and quantitative prediction of membrane chromatography: Extreme scale-up from 0.08 ml to 1200 ml. *J. Chromatogr. A*., *1332*, (2014), pp. 8-13.